Contrib Mineral Petrol (2002) 143: 438–449
DOI 10.1007/s00410-002-0355-8

Rais M. Latypov

Phase equilibria constraints on relations of ore-bearing intrusions with flood basalts in the Noril'sk region, Russia

Received: 10 February 2001 / Accepted: 20 January 2002 / Published online: 1 May 2002

Abstract Phase equilibria analysis has been performed to elucidate whether ore-bearing Noril'sk- and poorly mineralized Lower Talnakh-type intrusions are co-magmatic with the extremely Ni-, Cu- and PGEs-depleted and not depleted flood basalts, respectively. The parental magma of the intrusions is classified as silica-undersaturated olivine basalt, whereas that of the flood basalts is assigned to silica-saturated tholeiite. The plutonic equivalent of the former parental magma is olivine gabbro or melagabbro, whereas the latter is gabbronorite. Phase equilibria relations clearly show that these two types of magmas cannot be co-magmatic as there is no way to derive one liquid from another by fractional crystallization. This provides no support for the current model considering the Noril'sk-type intrusions as exit conduits for a great volume of volcanic magma, which lost most of its chalcophile elements in the shallow settling chambers on its way to surface. The association of a large volume of chalcophile element-depleted basalts with the very sulfide-rich intrusions in the Noril'sk region is most likely coincidental and cannot, therefore, be used as a regional criterion when prospecting for the Noril'sk-type sulfides deposits in other flood basalts provinces.

Introduction

The Ni–Cu deposits of the Noril'sk region are the third largest economic concentration of Ni in the world (after Sudbury, Canada, and Jinchuan, China) (Naldrett et al. 1992). They are also the world's largest repository of platinum group elements (PGEs) aside from the Bushveld Complex, South Africa. The mineralization of the Noril'sk region is associated with hypabyssal differentiated mafic/ultramafic intrusions subdivided into two groups: the ore-bearing Noril'sk- and poorly mineralized Lower Talnakh-type bodies (Fedorenko 1994a). These are intruded into sedimentary rocks immediately below the center of a 3.5-km-thick volcanic basin. Studies of overlying basalts have shown that basalts forming a 500-m-thick sequences (mostly Nadezhdinsky Formation) have lost 75% of their Cu and Ni, and more than 90% of their PGE (Naldrett 1997). This raised the question of whether the association of very sulfide-rich intrusions with a large volume of chalcophile element-depleted basalt has genetic significance (Naldrett 1994). The question has received two radically different interpretations.

Naldrett et al. (1995), following the earlier ideas of Godlevsky (1959) and Rad'ko (1991), put forward the concept of mineralized intrusions as exit conduits for 5,000–10,000 km^3 of volcanic magma. It was proposed that the sulfides precipitating from the first flow of contaminated basalt were trapped within the bodies of the Noril'sk-type intrusions, which acted as settling chambers at a shallow level in the crust. Subsequent magma flowing through these chambers interacted with the trapped sulfides, losing chalcophile elements and PGEs to the sulfides already present there. Thus, sulfides could interact with and concentrated metals from 5,000 to 10,000 times their own mass of magma that resulted in their present unusually metal-rich state. The poorly mineralized Lower Talnakh-type intrusions are also considered as exit conduits, with the only difference that magma flowing along them stopped much earlier than along those of the Noril'sk-type intrusions.

Czamanske et al. (1994) have rejected the idea of Naldrett et al. (1992) and Fedorenko (1994a) that the ores were derived in large part from the Cu-, Ni- and PGE-depleted overlying basalts. They found no obvious correlation between Pb and Sr initial isotopic ratios of

R.M. Latypov (✉)
Geological Institute, Kola Science Centre,
Apatity, 184200, Russia
E-mail: Rais.Latypov@oulu.fi
Tel.: +358-8-5531452
Fax: +358-8-5531484

Present address: R.M. Latypov
Institute of Geosciences, P.O. Box 3000,
University of Oulu, Finland

Editorial responsibility: I.S.E. Carmichael

the Noril'sk- and Lower Talnakh-type intrusions and those of basalts, and came to the conclusion that none of the intrusion-forming magmas can be directly related to any of the magmas that erupted as lavas. In addition, Czamanske et al. (1995) stressed that none of the apophyses to the ore-bearing intrusions are bordered by the expected thick hornfels selvages, i.e., there is no indication that truly vast amounts of magma exited the intrusion chambers. Another argument against the lava-conduit model is that there is little likelihood that the depletion in chalcophile elements and PGE that so uniformly characterize the voluminous Nadezhdinsky basalts (14,000 km^3) can be directly ascribed to processing in a rather small single chamber at the stratigraphic level of the ore-bearing intrusions (only 100 km^3 in volume; Czamanske et al. 1995).

The purpose of the present paper is to explore which of the two opposing points of view on the relations between Noril'sk- and Lower Talnakh-type intrusions and flood basalts is more consistent with the constraints provided by liquidus phase equilibria.

Geological background

The ore deposits of the Noril'sk region are located at the extreme northwestern margin of the Siberian Platform, Russia (Fig. 1). Within western Siberia, country rocks comprise marine and continental Silurian and Devonian sedimentary rocks overlain disconformably by the Middle Carboniferous to Late Permian lagoonal–continental and continental coal-bearing Tungusskaya series. The sedimentary sequence is covered by 2–3 million km^3 of late Permian and Triassic continental flood basalts and tuff known as the Siberian Trap. The Ni–Cu sulfide deposits are associated with a group of mafic–ultramafic intrusions, which are considered to be a part of the late Paleozoic to early Mesozoic episode of basaltic extrusion. The comprehensive information on geology, petrology, and geochemistry of the magmatic formations of the Noril'sk region can be found in numerous Russian and West publications summarized in Duzhikov and Distler (1992), and Lightfoot and Naldrett (1994). For the goals of the present paper, we describe below, in more detail, the stratigraphy and petrography of flood basalts and igneous stratigraphy of the ore-bearing intrusions.

Permo-Triassic volcanism

The volcanic sequence consists of a 3.5-km-thick alternating series of lavas and tuffs (ratio of lavas/tuffs = 9). The relative proportion of the volcanic rocks in the total of the Noril'sk magmatic rocks is about 95%, whereas mineralized intrusions constitute less than 0.01% (Fedorenko 1994a). The volcanic sequence of the Noril'sk region is divided into 11 suites on the basis of chemical composition and petrographic characteristics (Fedorenko 1994a). From lowermost to uppermost the suites are named Ivakinsky Formation (iv), Syverminsky Formation (sv), Gudchihinsky Formation (gd), Khakanchansky Formation (hk), Tuklonsky Formation (tk), Nadezhdinsky Formation (nd), Morongovsky Formation (mr), Mokulaevsky Formation (mk), Kharayelakhsky Formation (hr), Kumginsky Formation (km), and Samoedsky Formation (sm). Some formations are subdivided into subformations. In particular, the Nadezhdinsky Formation comprises from oldest to youngest nd_1, nd_2, and nd_3 subformations; the Morongovsky Formation includes mr_1 and mr_2 subformations. The petrography of the flood basalts includes abundant plagioclase phenocrysts (< 10 vol%) with lesser augite, and pseudomorphed olivine grains. The groundmass

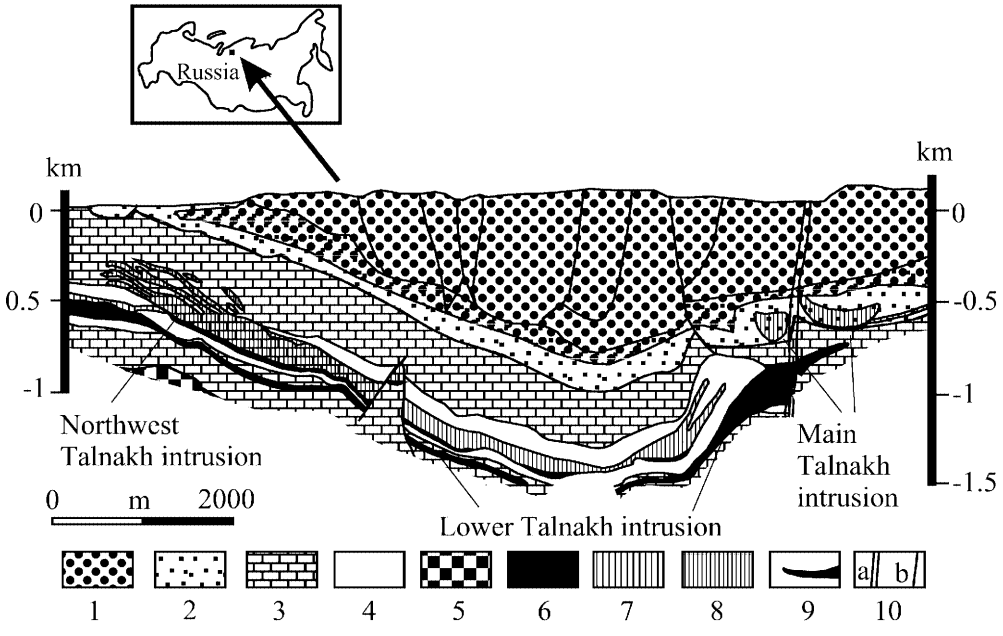

Fig. 1. Schematic longitudinal geologic cross section showing relationship between Main and Northwest Talnakh intrusions and Lower Talnakh intrusion (slightly modified from Naldrett et al. 1992). *1* Basalts (mr, nd, gd, sv, iv Formations); *2* Tungusskaya Series sedimentary rocks; *3* Devonian sediments above the Razvedochninsky and beneath the Kuzeysky Suites; *4* Devonian sediments of the Razvedochninsky and the Kuzeysky Suites; *5* Silurian sedimentary rocks; *6* Lower Talnakh intrusion; *7* Talnakh sill; *8* Northwest and Main Talnakh intrusions; *9* massive sulfide; *10 a* Noril'sk–Kharayelakh fault, *b* other faults

contains glass, anhedral grains of magnetite, and ilmenite needles (Lightfoot et al. 1993). Glass is universally present in the amount of 5–30 vol% in massive flow zones and up to 50 vol% and more in amygdaloidal lavas (Distler and Kunilov 1994).

Of most interest here are basalts of the Nadezhdinsky, Morongovsky, and Mokulaevsky Formations. Naldrett et al. (1995) emphasized the extremely Ni- and Cu-depleted nature of the contaminated basalts of the Nadezhdensky Formation (nd_1 and nd_2) from which it was suggested that ore-bearing intrusions have acquired chalcophile elements by sulfide segregation. On the basis of similarity of incompatible trace element abundances and isotopic ratios (REE profiles, Th/Ta–La/Sm diagram, Nd isotope ratios), Naldrett et al. (1992, 1995) concluded that the Nadezhdinsky lava is co-magmatic with the poorly mineralized Lower Talnakh-type intrusions, whereas the Mokulaevsky lava is co-magmatic with the ore-bearing Noril'sk-type intrusions. Fedorenko (1994a) supported this conclusion by demonstrating that the Lower Talnakh-type intrusions lie on a mixing line between Nadezhdinsky and Morongovsky magmas (mr_2) in terms of Th/U–Ce/Yb ratios whereas the Noril'sk-type intrusions are of Morongovsky magmas (mr_2). It is worthy of note that the conclusion about co-magmatic relations between basalts of nd, mr, and mk Formations and the Noril'sk- and Lower Talnakh-type intrusions is based principally on trace elements and isotope data; no major element evidence supporting this idea has been presented.

Ore-bearing Noril'sk-type intrusions

Ni–Cu mineralization is associated with differentiated bodies that are traced for more than 20 km as elongate sill-like bodies, 50 to 300 m thick and 500 to 2,000 m wide (Likhachev 1994). On the basis of field relationships, intrusions appear to be post-nd_2 and pre-mk in age (Naldrett et al. 1995). Fedorenko (1994a) subdivided them into two subgroups called Noril'sk- and Lower Talnakh-type intrusions. Significant mineralization is only associated with the Noril'sk-type intrusions displaying well-defined differentiation with picritic, olivine, and olivine-bearing gabbro–dolerite[1]. The Lower Talnakh type intrusions show weakly developed differentiation, with the section being dominated mostly by picritic gabbro–dolerite. The last type is poorly mineralized and does not constitute ore. It contains minor amount of sulfides with much lower Ni and Cu tenor and practically free of PGE. Figure 1 illustrates the manner in which poorly mineralized Lower Talnakh (Lower Talnakh-type) and ore-bearing Northwest and Main Talnakh intrusions (Noril'sk-type) lie with respect to each other, hosting sedimentary rocks and overlying flood basalts.

A schematic vertical section of a typical Noril'sk-type intrusion with modal percent of rock-forming minerals and appearance of liquidus phases is shown in Fig. 2. From the base upwards, the section is often subdivided into lower taxitic gabbro–dolerite (ol, 7–18%; pl, 45–72%; Cpx, 7–40%; opx, 0–1 %)[2], which is overlain by picritic gabbro–dolerite (ol, 40–80%; pl, 10–35%, Cpx, 5–25%, opx, 0.2–3 %, Cr-sp, 0–5%). This is followed, with decrease in the amount of olivine, by olivine gabbro–dolerite (ol, 10–27%, pl, 50–63%; Cpx, 10–20%; opx, $<2\%$), olivine-bearing gabbro–dolerite (ol, 3–7%; pl, 50–63%, Cpx, 20–30%, Cr-sp, 0–1%), prismatic gabbro (ol, 0–5%; pl, 45–65%, Cpx, 25–30%), magnetite gabbro (ol, 0–4%; pl, 45–65%, Cpx, 20–35%, mgt, 5–10%, opx, 0–3%), and leucogabbro (ol, 0–3%; pl, 75–80%; Cpx, 7–15%). Thus, the predominant minerals in the rocks of the Noril'sk-type intrusions are plagioclase, augite, and olivine. Orthopyroxene occurs here in a very subordinate amount (usually less than 1–2%). The Lower Talnakh-type intrusions are characterized by the same mineral composition (Distler et al. 1979).

In general, the internal stratigraphy of the Noril'sk-type intrusions is broadly predictable from in-situ differentiation of a single pulse of basic magma. Without considering a basal reversal in taxitic gabbro–dolerite, the overall trend of magma crystallization correlates well with the following sequence of phase appearance: Ol (1)→ Ol + Sp (2)→ Ol + Pl + Sp (3) → Ol + Pl (4)→ Ol + Pl + Cpx (5) → Ol + Pl + Cpx + Mgt (6)→ Ol + Pl + Cpx + Opx (7) (Likhachev 1965, 1977; Nekrasov and Gorbachev 1978; Zen'ko 1983; Fig. 2). The stages are consistent with the crystallization of the following rock types: 1 and 2 – picritic gabbro–dolerite, 3 and 4 – olivine gabbro–dolerite, 5 – olivine-bearing gabbro–dolerite and prismatic gabbro, 6 – magnetite gabbro, and 7 – orthopyroxene-bearing intercumulus material within cumulate rocks. Marakushev et al. (1982), Ryabov (1992), Fedorenko (1994b), and Czamanske et al. (1995) disagree with the single input model and reason that the Noril'sk-type intrusions are more likely to have formed by sequential introduction of several distinct but very closely related magma types. In the present discussion I will adhere to the single input model because it seems to me more reasonable (Latypov, in preparation). Actually, it is equally possible here to consider the intrusion's formation in the frame of the multiple intrusion model because the choice between these opposing models has little effect on the overall conclusion of our investigation.

Methods of investigation

For the following analysis we use a slightly modified isobaro-isoplethic section of the six-component system

[1] The name "gabbro–dolerite" is firmly entrenched in the literature of Noril'sk. The usage was established because subvolcanic intrusions contain rocks that are too coarse grained to be properly called dolerites. See detail clarification of this term in Czamanske et al. (1995).

[2] Hereinafter, mineral modal abundances are reported on the basis of Czamanske et al. (1995) and Likhachev (1994).

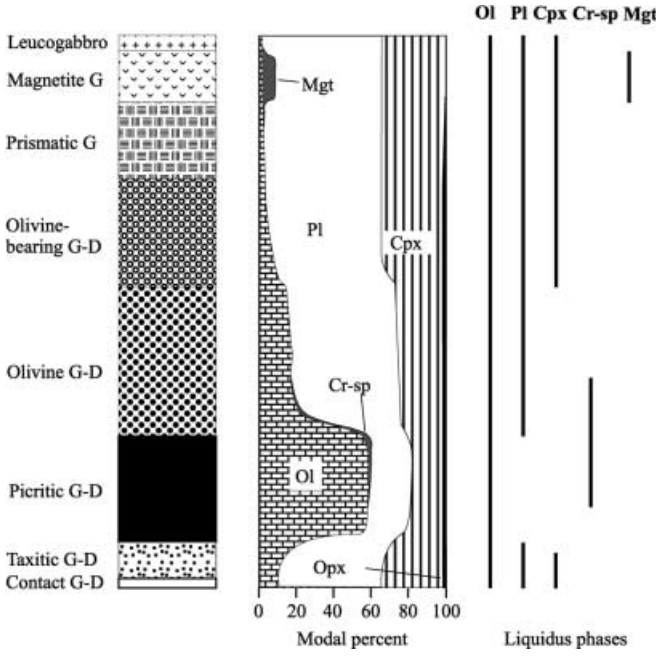

Fig. 2. Schematic cross section of a typical Noril'sk-type intrusion showing vertical variation in modal abundances of rock-forming minerals and appearance of liquidus (cumulus) phases. The cross section is based mainly on Czamanske et al. (1995), Distler et al. (1979), Zolotukhin et al. (1975), and Zen'ko (1983). *G* Gabbro; *G-D* gabbro–dolerite

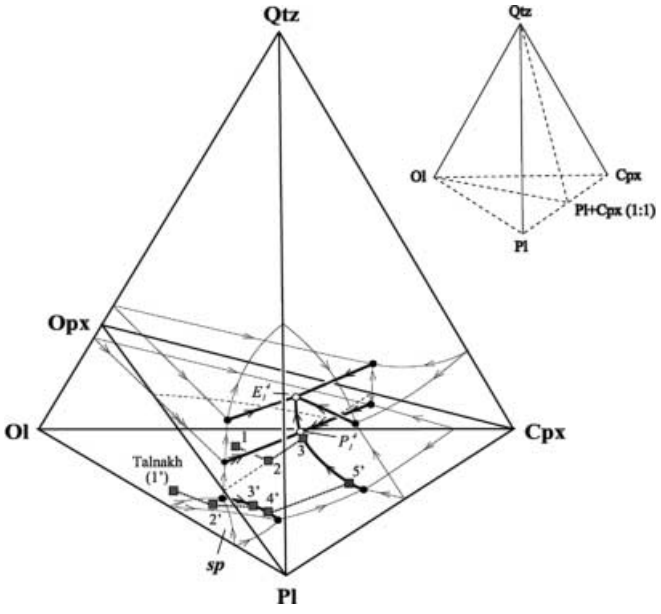

Fig. 3. Phase relations along the isobaro-isoplethic section Ol–Cpx–Pl–Qtz (mg# 50–75; An = 60–70) at P < 1,000 bar, with compositions of the components expressed in wt% (slightly modified from Dubrovskii 1998). *Thick solid curves* indicate liquidus lines within the Ol–Cpx–Pl–Qtz tetrahedron; *thin curves* are liquidus lines on the faces of the tetrahedron. Invariant points in the interior of the tetrahedron are shown as *open circles*. *Filled circles* represent ternary points on the faces of the tetrahedron. *Two dashed, fine lines* illustrate the intersection of the divariant surfaces Ol–Opx–L, Ol–Pl–L, Ol–Cpx–L, and Opx–Cpx–L with the silica-saturation plane Opx–Cpx–Pl. Hereafter, cotectic and reaction lines are indicated by one and two *arrows*, respectively. *Arrows* point toward decreasing temperature. Also shown are generalized fractionation trends for the parental magmas of the ore-bearing Talnakh intrusion (1′–2′–3′–4′–5′ and flood basalts (1–2–3). The position of two projection planes, Ol–Qtz–(Pl + Cpx) and (Ol + Opx)–Cpx–Pl, used in this paper for plotting compositional points is shown in the *top right corner*. E_1^4 – Qtz + Opx + Cpx + Pl = L; P_1^4 – Opx + Cpx + Pl = L + Ol

Fo–Fa–Di–Hd–Ab–An–Qtz (Fig. 3). This has been developed graphically by Dubrovskii (1993, 1998) using a standard approach for graphical analysis of phase equilibria, given in the works of Schreinemakers (1965), Ricci (1951), Korzhinskii (1959), and Ehlers (1972). The choice of the isobaro-isoplethic section Ol–Cpx–Pl–Qtz (mg# = 50–75; An = 60–70) has been made on the basis of normative plagioclase and olivine composition in the rocks of the mineralized intrusions and flood basalts (Tables 1, 2, 3, 4, 5, and 6). The silica-saturation plane Opx–Cpx–Pl separates the Ol–Cpx–Pl–Qtz tetrahedron into two isoplethic sections: a quartz-normative section, Opx–Cpx–Pl–Qtz, and an olivine-normative section, Ol–Opx–Cpx–Pl. The system contains two isobaric invariant points: eutectic point E_1^4, Qtz + Opx + Cpx + Pl = L, and a piercing point P_1^4, Opx + Cpx + Pl = L + Ol. The complexity of the graphic representation of the diagram makes it difficult to use the isobaro-isoplethic section in solving petrological tasks. That is why simplified projections of the isobaro-isoplethic section on two triangular planes, Ol–Qtz–(Pl + Cpx) and (Ol + Opx)–Cpx–Pl (Fig. 3, upper inset), were used as proposed by Dubrovskii (1998). These planes were chosen in order to avoid distortion of the mutual position of topology elements and rock composition points; such distortion often occurs when compositional points are projected from a tetrahedron onto its triangular faces.

Extensive geochemical data used in this paper has been extracted from the following sources: Talnakh intrusion (Zolotukhin et al. 1975; Czamanske et al. 1994, 1995), Lower Talnakh intrusion (Czamanske et al. 1994), basalts of the Nadezhdinsky, Morongovsky, and Mokulaevsky Formations (Lightfoot et al. 1990), average compositions of some Noril'sk- and Lower Talnakh-type intrusions and basalt Formations (Duzhikov and Strunin 1992), and average compositions of the Irbinsky and Ambarninsky dolerite intrusions (Fedorenko et al. 1984). All whole-rock analyses have been recalculated to CIPW norms, which were used then for plotting on the projection planes. The technical aspects of the plotting are given in Appendix B. Because of more intensive alteration, basalts are commonly characterized by much higher Fe^{3+}/Fe^{2+} ratios than intrusive rocks (0.45–0.90 and 0.20–0.70, respectively). To avoid distortions of CIPW norms caused by high oxidation state of volcanic rocks, all basalts analyses were calculated with the standard ratio $Fe^{3+}/Fe^{2+} = 0.20$ which is close to that recommended for basalts by Brooks (1976). No corrections of Fe^{3+}/Fe^{2+} ratios for intrusive rocks have been deliberately made to preclude the possibility that compositional difference between basalts and intrusive rocks

Table 1. Chemical (wt%) and CIPW normative compositions of the ore-bearing Northwest Talnakh intrusion, borehole KZ-1879 (data from Czamanske et al. 1994, with Fe^{3+}/Fe^{2+} ratio from Likhachev 1994). *Go* Olivine gabbro–dolerite; *Gob* olivine-bearing gabbro–dolerite; *Gp* picritic gabbro–dolerite; *Lg* leucogabbro. An(norm) = 100*An/(An + Ab); Mg# = 100*Mg/(Mg + Fe^{2+} + Fe^{3+}). fsp = or + ab + an

Rock	Lg	Lg	Gob	Gob	Gob	Gob	Gob	Gob	Go	Go
SiO_2	46.10	45.10	46.80	46.20	45.60	45.70	46.40	46.00	45.40	44.60
TiO_2	0.56	0.33	0.55	0.64	0.67	0.60	0.59	0.56	0.47	0.45
Al_2O_3	23.00	23.00	15.50	15.90	13.80	14.90	17.60	17.30	15.80	14.40
Fe_2O_3	1.40	1.48	1.92	1.70	2.51	1.77	2.20	1.65	1.75	1.79
FeO	5.75	5.35	6.81	8.00	8.08	8.56	7.00	7.46	8.22	9.00
MnO	0.15	0.16	0.17	0.18	0.21	0.20	0.14	0.14	0.16	0.18
MgO	3.72	6.06	11.30	11.80	14.10	13.50	11.80	12.50	14.80	17.00
CaO	10.30	11.60	12.70	11.30	10.30	10.80	11.20	11.00	10.20	9.30
Na_2O	1.96	1.86	1.52	1.64	1.43	1.41	1.69	1.63	1.48	1.31
K_2O	2.76	1.21	0.43	0.37	0.43	0.38	0.28	0.25	0.21	0.31
P_2O_5	0.08	0.06	0.06	0.08	0.08	0.07	0.07	0.07	0.06	0.05
H_2O^+	3.72	3.62	2.20	1.92	1.88	1.73	1.29	1.24	1.27	1.51
H_2O^-	0.10	0.47	0.21	0.17	0.25	0.17	0.13	0.13	0.13	0.21
S	0.29	0.23	0.04	0.06	0.06	0.06	0.05	0.05	0.04	0.04
CO_2	0.13	0.19	0.01	0.06	0.06	0.03	0.06	0.04	0.03	0.04
Total	100.02	100.72	100.22	100.02	99.46	99.88	100.50	100.02	100.02	100.19
cc	0.30	0.43	0.02	0.14	0.14	0.07	0.14	0.09	0.07	0.09
ap	0.19	0.14	0.14	0.19	0.19	0.17	0.17	0.17	0.14	0.12
ilm	1.06	0.63	1.05	1.22	1.27	1.14	1.12	1.06	0.89	0.86
mgt	2.03	2.15	2.79	2.47	3.64	2.57	3.19	2.39	2.54	2.60
pr	0.54	0.43	0.07	0.11	0.11	0.11	0.09	0.09	0.07	0.07
fsp	75.34	73.72	49.59	50.99	44.60	47.38	55.55	54.42	49.61	45.41
cpx		0.58	5.80	7.19	10.45	7.87	8.52	7.00	6.86	5.56
cpx		4.10	22.75	16.29	16.20	15.87	12.11	11.81	11.37	10.46
ol	11.61	13.39	15.58	19.33	20.71	22.80	18.18	21.62	27.07	33.29
ne	1.82									
An(norm)	76.56	75.28	71.49	70.36	70.02	72.41	72.32	72.80	72.97	73.44
Mg#	48.60	65.52	70.22	68.81	70.85	70.32	70.07	71.35	72.92	74.06

Table 2. Chemical (wt%) and CIPW normative compositions of the ore-bearing Northwest Talnakh intrusion, borehole KZ-1879 (data from Czamanske et al. 1994, with Fe^{3+}/Fe^{2+} ratio from Likhachev 1994). *Go* Olivine gabbro–dolerite; *Gob* olivine-bearing gabbro–dolerite; *Gp* picritic gabbro–dolerite; *Lg* leucogabbro. An(norm) = 100*An/(An + Ab); Mg# = 100*Mg/(Mg + Fe^{2+} + Fe^{3+}). fsp = or + ab + an

Rock	Gob	Gob	Gp	Gp	Gp	Gp	Go	Gp	Go	Go	Gob
SiO_2	45.60	46.80	35.90	38.40	38.00	40.50	42.70	42.20	45.10	44.30	39.50
TiO_2	0.48	0.54	0.43	0.37	0.36	0.51	0.59	0.56	0.89	0.87	0.79
Al_2O_3	17.30	18.60	6.12	5.71	5.66	7.20	13.00	7.46	13.00	11.90	12.40
Fe_2O_3	1.78	1.62	7.91	6.45	5.70	5.44	3.41	4.41	3.71	3.54	9.48
FeO	7.20	7.17	10.32	9.21	9.88	9.31	10.23	10.23	8.62	10.48	10.79
MnO	0.14	0.14	0.21	0.20	0.21	0.20	0.17	0.22	0.18	0.20	7.09
MgO	13.00	10.20	23.00	25.30	24.90	23.80	15.40	24.00	14.40	14.70	0.33
CaO	11.00	12.10	4.50	4.36	3.50	5.49	7.85	5.85	8.63	8.18	7.08
Na_2O	1.57	1.70	0.75	0.69	0.60	0.92	1.52	1.08	1.74	1.47	2.36
K_2O	0.20	0.25	0.11	0.14	0.12	0.17	0.48	0.22	0.48	0.83	0.59
P_2O_5	0.06	0.06	0.06	0.05	0.05	0.06	0.07	0.08	0.11	0.10	0.09
H_2O^+	1.57	0.79	6.08	7.11	8.60	4.85	1.94	3.07	1.59	1.68	4.00
H_2O^-	0.21	0.12	0.37	0.43	0.69	0.33	0.21	0.21	0.27	0.11	0.73
S	0.03	0.04	2.90	1.32	1.22	0.95	2.08	0.23	1.33	1.12	4.49
CO_2	0.17	0.09	0.94	0.34	0.17	0.44	0.07	0.56	0.25	0.53	0.08
Total	100.31	100.22	99.60	100.08	99.66	100.17	99.72	100.38	100.30	100.01	99.80
cc	0.39	0.20	2.14	0.77	0.39	1.00	0.16	1.27	0.57	1.21	0.18
ap	0.14	0.14	0.14	0.12	0.12	0.14	0.17	0.19	0.26	0.24	0.21
ilm	0.91	1.03	0.82	0.70	0.68	0.97	1.12	1.06	1.69	1.65	1.50
mgt	2.58	2.35	11.47	9.36	8.27	7.89	4.95	6.40	5.38	5.13	13.75
pr	0.06	0.07	5.43	2.47	2.28	1.78	3.89	0.43	2.49	2.10	8.40
fsp	54.03	58.24	20.00	18.74	18.18	23.80	42.92	25.29	43.81	40.75	44.95
cpx	7.18	7.68	20.57	19.07	22.73	17.47	9.84	15.05	15.60	15.37	15.07
cpx	10.85	13.44	2.34	5.59	2.82	7.15	8.63	8.03	11.36	10.55	9.86
ol	22.38	16.14	29.53	35.40	34.60	34.54	25.38	39.32	16.97	20.95	
ne											
An(norm)	73.74	73.53	65.90	66.10	69.72	64.52	66.63	60.53	62.70	63.97	50.38
Mg#	72.46	67.81	70.15	75.02	74.72	74.91	67.36	75.07	68.21	65.71	39.54

can arise from arbitrary choice of oxidation state of intrusive rocks. Representative analytical data, along with the CIPW norms for the Talnakh intrusion (KZ-1879), basalts of nd, mr, and mk Formations, and average compositions of some intrusions and basalt formations are listed in Tables 1, 2, 3, 4, 5, and 6.

Phase equilibria analysis

One important distinction in the location of rocks of the Talnakh and Lower Talnakh-type intrusions and basalts of nd, mr, and mk Formations stands out on the pro-

Table 3. Chemical (wt%) and CIPW normative compositions of basalts from Mokulaevsky (*mk*), Morongovsky (*mr*), and Nadezhdinsky (*nd*) Formations (data from Lightfoot et al. 1990). Norms were calculated using the atomic ratio $Fe^{3+}/Fe^{2+} = 1/5$. An (norm) = 100*An/(An + Ab); Mg# = 100*Mg/(Mg + Fe^{2+} + Fe^{3+}). *LOI* Loss on ignition; *fsp* or + ab + an

Formation	mk	mk	mk	mk	mk	mk	mk	mk	mk	mr
SiO_2	48.30	48.50	48.20	48.50	48.70	49.10	48.90	49.10	48.90	48.90
TiO_2	1.33	1.29	1.19	1.22	1.22	1.21	1.11	1.19	1.15	1.12
Al_2O_3	16.42	15.59	17.51	17.21	16.08	16.24	16.59	15.78	16.46	16.73
Fe_2O_3	13.36	13.52	12.49	12.66	13.22	12.71	12.54	12.79	12.49	12.27
MgO	6.83	7.28	6.78	6.81	6.64	6.63	7.03	6.56	6.89	7.15
MnO	0.18	0.21	0.20	0.18	0.20	0.19	0.19	0.18	0.19	0.19
CaO	11.02	11.04	11.37	10.65	11.68	11.60	11.03	12.17	11.78	11.35
Na_2O	2.17	2.06	1.95	1.97	1.99	2.02	2.18	1.96	1.90	1.98
K_2O	0.23	0.37	0.17	0.75	0.22	0.20	0.36	0.18	0.17	0.25
P_2O_5	0.10	0.12	0.11	0.09	0.09	0.10	0.10	0.10	0.11	0.10
Total	99.94	99.98	99.97	100.04	100.04	100.00	100.03	100.01	100.04	100.04
LOI	1.40	3.00	1.60	1.40	2.20	0.80	1.20	3.00	1.40	0.80
ap	0.24	0.28	0.26	0.21	0.21	0.24	0.24	0.24	0.26	0.24
ilm	2.53	2.45	2.26	2.32	2.32	2.30	2.11	2.26	2.19	2.13
mt	3.23	3.28	5.44	5.51	5.76	5.54	5.47	5.57	5.44	5.34
fsp	54.10	51.81	56.01	56.99	52.43	52.92	54.99	51.37	52.95	54.26
opx	19.43	19.91	21.77	19.19	21.52	21.59	19.40	20.00	22.27	22.67
cpx	16.15	17.90	14.10	13.42	19.00	18.29	16.13	21.39	17.94	16.09
ol	3.40	3.23	1.51	3.79	0.28		3.11			0.68
qu						0.53		0.60	0.38	
An (norm)	63.85	63.53	68.77	67.01	65.76	65.66	63.76	65.73	67.79	66.97
Mg#	50.29	51.59	51.79	51.56	49.85	50.81	52.59	50.37	52.19	53.57

Table 4. Chemical (wt%) and CIPW normative compositions of basalts from Mokulaevsky (*mk*), Morongovsky (*mr*), and Nadezhdinsky (*nd*) Formations (data from Lightfoot et al. 1990). Norms were calculated using the atomic ratio $Fe^{3+}/Fe^{2+} = 1/5$. An (norm) = 100*An/(An + Ab); Mg# = 100*Mg/(Mg + Fe^{2+} + Fe^{3+}). *LOI* Loss on ignition; *fsp* or + ab + an

Formation	mr	mr	mr	mr	mr	mr	mr	mr	mr	mr	nd
SiO_2	48.90	48.90	48.80	49.10	48.40	49.60	49.70	49.70	49.90	50.10	49.50
TiO_2	1.14	1.12	1.11	1.14	1.12	1.27	1.00	1.05	1.03	0.84	1.09
Al_2O_3	17.07	16.21	17.00	16.29	17.33	16.32	15.83	15.51	16.44	17.84	17.28
Fe_2O_3	11.79	12.94	12.22	12.50	12.64	12.75	12.54	12.45	11.51	10.91	11.79
MgO	7.18	7.19	7.25	7.22	6.98	5.79	7.31	7.07	7.05	6.15	6.75
MnO	0.17	0.20	0.18	0.19	0.19	0.18	0.17	0.18	0.16	0.17	0.17
CaO	11.48	10.91	11.10	11.16	11.01	11.33	11.20	11.53	11.51	10.91	10.78
Na_2O	1.92	1.93	1.88	2.05	1.98	2.02	1.80	1.92	1.95	2.08	2.01
K_2O	0.24	0.46	0.36	0.28	0.20	0.62	0.33	0.51	0.32	0.92	0.50
P_2O_5	0.11	0.12	0.12	0.11	0.10	0.13	0.09	0.11	0.10	0.14	0.12
Total	100.00	99.98	100.02	100.04	99.95	100.01	99.97	100.03	99.97	100.06	99.99
LOI	1.60	1.80	1.60	1.60	1.80	1.00	2.40	1.80	2.60	1.90	1.60
ap	0.26	0.28	0.28	0.26	0.24	0.31	0.21	0.26	0.24	0.33	0.28
ilm	2.17	2.13	2.11	2.17	2.13	2.41	1.90	2.00	1.96	1.60	2.07
mt	5.13	5.64	5.32	5.44	5.51	5.56	5.47	5.42	5.02	4.76	5.13
fsp	54.91	53.25	54.92	53.41	55.74	54.37	51.31	51.45	53.54	59.66	56.60
opx	23.30	23.53	23.94	22.93	23.00	19.56	24.01	21.83	21.87	21.05	23.46
cpx	15.53	15.71	14.25	16.59	13.27	17.95	17.08	19.93	17.42	13.62	13.16
ol		0.89	0.56	0.63	1.48						
qu	0.01					1.26	1.37	0.52	1.21	0.27	0.58
An (norm)	68.38	66.39	68.62	65.17	68.03	64.98	67.88	65.14	66.77	66.24	67.02
Mg#	54.65	52.37	54.00	53.34	52.22	47.34	53.56	52.90	54.79	52.73	53.12

jection planes in Fig. 4. The rocks of the intrusions, falling mostly within the olivine-normative section Ol–Cpx–Opx–Pl, gravitate towards the critical Ol–Cpx–Pl plane of silica undersaturation as would be expected from their nearly opx-free composition. In contrast, the basalts of nd, mr, and mk Formations define a rather compact field near to the critical Opx–Cpx–Pl plane of silica saturation, with some points of nd formations lying well within the quartz-normative section Qtz–Cpx–Opx–Pl (Fig. 4). The shift of some compositional points of picritic, picritic-like, and olivine gabbro–dolerite (Fig. 4) from their original position near to the joint Ol–(Pl + Cpx) towards the Opx apex is clearly related to the high content of metamorphically produced normative orthopyroxene. Normative orthopyroxene usually arises because of the development of serpentine, talc, and chlorite, containing some molecules of orthopyroxene in their composition, after olivine. The displacement of some rocks of the residual sequence, namely, olivine-bearing gabbro–dolerite (Fig. 4a–c), prismatic and magnetite gabbro (Fig. 4b) towards the join Opx–(Pl + Cpx) is likely connected with their contamination or/and post-magmatic alteration. The involvement of contamination in their genesis is supported by the common occurrence of quartz in these rocks and their close association with quartz diorite, which is interpreted as a hybrid rock type highly contaminated by host rocks (Czamanske et al. 1995). The contaminated nature of quartz diorite is supported by its location near to the joint Qtz–(Pl + Cpx), which is far beyond the position

Table 5. Chemical (wt%) and CIPW normative compositions of basalts from Mokulaevsky (*mk*), Morongovsky (*mr*), and Nadezhdinsky (*nd*) Formations (data from Lightfoot et al. 1990). Norms were calculated using the atomic ratio $Fe^{3+}/Fe^{2+} = 1/5$. An (norm) = 100*An/(An + Ab); Mg# = 100*Mg/($Mg + Fe^{2+} + Fe^{3+}$). *LOI* Loss on ignition; *fsp* or + ab + an

Formation	nd	nd	nd	nd	nd	nd	nd	nd	nd	nd
SiO_2	50.00	55.20	52.70	51.20	51.20	51.20	49.40	53.40	53.30	52.10
TiO_2	1.14	1.07	1.01	0.96	0.83	1.00	0.91	0.95	0.92	0.93
Al_2O_3	16.43	15.33	15.61	17.49	16.37	16.62	20.86	15.93	15.99	16.23
Fe_2O_3	12.50	10.66	11.25	10.47	10.43	10.35	9.91	10.11	9.96	10.31
MgO	6.28	5.25	5.28	6.35	6.60	5.91	5.93	5.44	6.57	6.29
MnO	0.19	0.16	0.16	0.15	0.14	0.15	0.14	0.15	0.16	0.16
CaO	11.16	8.52	9.98	10.07	11.57	11.89	9.79	8.77	10.18	10.82
Na_2O	1.76	2.54	2.13	2.05	2.66	2.64	2.01	3.18	2.48	2.05
K_2O	0.44	1.16	1.22	1.21	0.14	0.12	0.96	1.92	0.40	1.04
P_2O_5	0.11	0.11	0.10	0.09	0.08	0.08	0.07	0.10	0.07	0.09
Total	100.01	100.00	99.44	100.04	100.02	99.96	99.98	99.95	100.03	100.02
LOI	3.00	1.40	1.00	1.00	4.00	4.60	1.20	2.80	4.00	1.00
ap	0.26	0.26	0.24	0.21	0.19	0.19	0.17	0.24	0.17	0.21
ilm	2.17	2.03	1.92	1.82	1.58	1.90	1.73	1.81	1.75	1.77
mt	5.44	4.64	4.90	4.55	4.54	4.51	4.32	4.41	4.34	4.50
fsp	53.11	55.34	54.65	59.44	55.65	56.19	67.73	61.76	54.65	55.49
opx	21.87	18.90	17.79	21.69	18.39	15.96	24.57	16.96	20.00	18.74
cpx	15.66	11.98	16.04	11.80	20.09	20.76	2.49	15.89	15.29	17.26
ol										
qu	2.88	8.03	5.16	1.68	0.74	1.60	0.07	0.02	4.94	3.21
An (norm)	69.29	54.23	60.63	65.52	57.52	58.32	71.42	45.19	58.46	63.51
Mg#	49.86	49.35	48.15	54.55	55.61	53.05	54.22	51.56	56.62	54.68

Table 6. Average chemical (wt%) and CIPW normative compositions of dolerite intrusions (data from Fedorenko et al. 1984), nd, mr, and mk volcanic formations, ore-bearing Noril'sk (T, N-I, N-I') and poorly mineralized Lower Talnakh type (L-T, L-N, L-TT, Kl, Zel, Mor) intrusions (data from Duzhikov and Strunin 1992). Intrusions: *T* Talnakh; *N-I* Noril'sk; *N-I'* Eastern Noril'sk branch of the Noril'sk intrusion; *L-N* Lower Noril'sk; *L-T* Lower Talnakh; *Kl* Klukvenny; *Mor* Morongo; *L-TT* Lower Tulaek-Taassky; *Zel* Zelyonaya Griva. Dolerite intrusions: *Ir1*, *Ir2* Irbinsky type; *Am1*, *Am2* Ambarninsky type. Volcanic formations: *nd* Nadezhdinsky; *mr* Morongovsky; *mk* Mokulaevsky. Analytical data for the Talnakh intrusion (*T*) is from Zolotukhin et al. (1975). An (norm) = 100*An/(An + Ab); Mg# = 100*Mg/($Mg + Fe^{2+} + Fe^{3+}$). *LOI* Loss on ignition. fsp = or + ab + an. Norms for nd, mr, and mk Formations were calculated using the atomic ratio $Fe^{3+}/Fe^{2+} = 1/5$

	nd	mr	mk	Ir1	Ir2	Am1	Am2	T	N-I	N-I'	L-T	L-N	L-TT	Kl	Zel	Mor
SiO_2	49.48	48.63	48.20	48.56	49.94	48.12	47.20	43.40	45.21	45.25	44.69	42.71	44.47	44.52	45.10	44.01
TiO_2	1.07	1.16	1.25	1.06	1.04	1.34	1.54	0.96	0.66	0.79	0.79	0.70	0.88	0.59	0.72	0.78
Al_2O_3	15.87	15.26	15.24	15.07	15.28	15.25	15.54	14.47	14.02	14.35	12.99	9.63	13.31	11.19	14.10	14.20
Fe_2O_3	4.60	4.68	4.53	2.96	2.38	3.25	3.59	3.74	3.54	2.37	2.63	3.31	2.90	3.01	1.83	1.92
FeO	5.89	7.37	7.86	8.19	8.04	8.99	9.59	9.24	8.13	8.58	8.37	9.45	12.42	9.22	9.84	11.74
MnO	0.16	0.18	0.20	0.17	0.16	0.21	0.23	0.18	0.15	0.16	0.19	0.25	0.20	0.19	0.23	0.18
MgO	5.92	7.43	7.23	8.31	7.07	7.07	7.62	11.39	12.29	11.65	13.75	20.10	14.34	17.56	13.60	15.37
CaO	11.40	10.86	10.88	11.03	10.56	10.71	10.00	9.16	9.82	10.64	9.07	7.13	8.21	7.84	9.21	8.06
Na_2O	2.50	1.99	2.00	2.07	2.15	2.27	2.20	1.74	1.73	1.89	1.51	0.97	1.74	1.38	1.05	1.57
K_2O	0.67	0.45	0.45	0.50	0.92	0.51	0.44	0.88	0.48	0.39	0.76	0.78	0.49	0.54	1.16	0.30
P_2O_5	0.23	0.15	0.15	0.10	0.14	0.17	0.16	0.14	0.10	0.13	0.12	0.09	0.15	0.08	0.12	0.10
LOI	1.89	1.82	2.01	1.75	2.20	2.00	1.83	3.58	2.89	2.83	4.43	3.44	1.04	3.90	3.34	1.54
Total	99.70	100.01	100.01	99.77	99.88	99.89	99.94	98.88	99.2	99.15	99.31	98.61	100.17	100.03	100.30	99.81
ap	0.54	0.36	0.36	0.24	0.33	0.40	0.38	0.33	0.24	0.31	0.28	0.21	0.36	0.19	0.28	0.24
ilm	2.03	2.20	2.38	2.01	1.98	2.55	2.93	1.82	1.25	1.50	1.5	1.33	1.67	1.12	1.37	1.48
mt	6.67	6.79	6.57	4.29	3.45	4.71	5.21	5.42	5.13	3.44	3.81	4.80	4.21	4.37	2.65	2.79
fsp	55.21	50.87	50.85	50.81	52.95	52.13	52.44	49.00	46.54	47.80	43.68	32.43	44.67	37.61	46.07	45.86
en	7.74	12.67	12.32	12.08	12.25	10.78	11.35	2.50	7.62	2.95	7.37	7.07	3.80	8.96	7.44	4.60
fs	2.91	5.54	6.16	6.52	7.92	7.35	7.5	1.12	2.79	1.30	2.64	1.97	2.06	2.83	3.47	2.29
opx	10.65	18.21	18.48	18.60	20.17	18.13	18.85	3.62	10.41	4.25	10.01	9.04	5.86	11.79	10.91	6.89
cpx	20.04	17.35	17.57	19.23	18.06	18.05	14.14	12.46	15.25	18.08	14.27	12.10	10.29	12.50	11.76	6.89
ol				2.84		1.93	4.18	22.66	19.36	20.83	21.32	35.21	32.06	28.55	23.91	34.10
qu	2.66	2.40	1.79		0.77											
An (norm)	57.30	63.73	63.54	62.04	60.32	59.50	61.27	65.06	65.19	63.51	66.1	69.27	63.41	64.75	76.30	68.63
Mg#	51.26	53.34	51.91	57.70	55.30	51.39	51.43	61.69	65.93	65.96	69.53	74.24	62.96	72.40	67.84	67.03

of the main field of compositional points of the Talnakh intrusion (Fig. 4b).

The same difference in location of the intrusions and basalts on the projection planes is evident from comparison of their average compositions (Fig. 5). The intrusions lie close to the critical Ol–Cpx–Pl plane of silica undersaturation whereas volcanic formations are located near to the critical Opx–Cpx–Pl plane of silica saturation. From this, it follows immediately that the products of the equilibrium crystallization of the parental magmas of the intrusions and the basalts will be considerably different. The former will complete

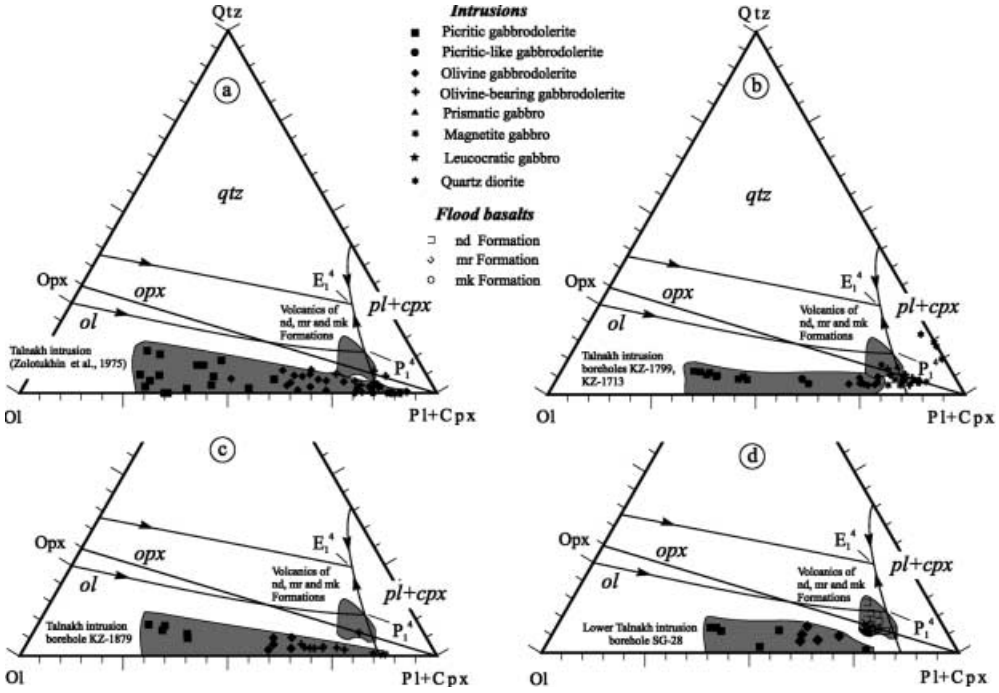

Fig. 4a–d. Projection planes of the isobaro-isoplethic section Ol–Cpx–Pl–Qtz showing fields with rocks of the Talnakh and Lower Talnakh intrusions and basalts of the nd, mr, and mk Formations. All analytical data for the boreholes KZ-1879 (Tables 1, 2), KZ-1799, KZ-1713 of the Talnakh intrusion and a borehole SG-28 of the Lower Talnakh intrusion are taken from Czamanske et al. (1994, 1995). The Fe^{3+}/Fe^{2+} ratios for these data are kindly provided by V.A. Fedorenko. Analytical data for the basalts of the nd, mr, and mk Formations are taken from Lightfoot et al. (1990) and are listed in Tables 3, 4, and 5

crystallization with the formation of three-phase Pl + Cpx + Ol paragenesis of olivine gabbro (Noril'sk-type intrusions), or olivine melagabbro (Lower Talnakh-type intrusions). The latter will produce a three-phase Pl + Cpx + Opx paragenesis of gabbronorite. The field of typical fresh gabbronorites (Pl–Opx–Cpx cumulates) of the West Pansky Tundra layered intrusions (Fig. 5c) is nearly overlapped with that of the basalts under investigation.

The conclusion about Pl + Cpx + Opx composition of basalts seems to be at odds with the petrographic observations showing that the bulk of all volcanic rocks and related intrusions is similar and composed of three major silicates: plagioclase, augite, and olivine (e.g., Distler and Kunilov 1994). This similarity, however, can have a quite simple explanation. Because of incongruent melting of orthopyroxene, both the parental magmas of intrusions and basalts fall within the primary volume of olivine (Fig. 4), which permits them to follow nearly the same crystallization sequence despite significant difference in composition (Fig. 3). Let us consider, for example, the crystallization path of a parental magma of the Talnakh intrusion. As its average composition lies within an olivine volume, the crystallization will start with precipitation of olivine (point 1′ in Fig. 3). This stage correlates with the formation of a picritic gabbro–dolerite layer (Fig. 2). Upon further evolution, the liquid moves away from the Ol apex. On this path, olivine is joined subsequently by Cr-spinel (a path from 2′ to 3) and plagioclase (a path from 3′ to 4′), with the following peritectic disappearance of Cr-spinel and co-crystallization of olivine and plagioclase along the cotectic plane Ol + Pl = L (a path from 4′ to 5′). The stages from 3′ to 5′, corresponding to the formation of olivine gabbro–dolerite, will be marked by an abrupt decrease in the amount of olivine because the proportions of olivine to plagioclase that crystallize cotectically in basaltic systems is typically about 25:75 (Morse 1979). With further cooling, the liquid reaches the cotectic line Ol + Pl + Cpx = L where fractional assemblage is joined by augite (point 5' in Fig. 3). Here, the modal abundances of olivine in the assemblage will further decrease as cotectic proportions of olivine to plagioclase and augite is about 10:60:30 (Osborn and Tait 1952; Dubrovskii 1998). The crystallization along the line Ol + Pl + Cpx = L is consistent with formation of the residual sequence composed of olivine-bearing gabbro–dolerite, prismatic and magnetite gabbro (Fig. 2).

In general, during most of the crystallization period, the melt will be localized close to a silica-undersaturated critical plane Ol–Pl–Cpx following the order of phase crystallization: Ol (1′–2′) → Ol + Sp (2′–3′) → Ol + Pl + Sp (3′–4′) → Ol + Pl (4′–5′) → Ol + Pl + Cpx (5′–P_1^4) → Ol + Pl + Cpx + Opx (P_1^4). Only a small amount of the trapped liquid within cumulates is able to reach an isobaric invariant point P_1^4 (Cpx + Opx + Pl = L + Ol), as it is evident from the minor content of orthopyroxene in the rocks (Fig. 2). As for the Lower Talnakh-type intrusions, the order of phase crystallization of their parental magmas must be principally identical to that of the Noril'sk-type intrusions. The only difference is that a layer of picritic gabbro–dolerite in the former will be much thicker because their parental magmas are richer in normative olivine (Fig. 5).

The crystallization of flood basalts will also start with precipitation of olivine (point 1 in Fig. 3), which will be subsequently accompanied by plagioclase (a path from 2 to 3) and clinopyroxene (a path from 3 to P_1^4). Most

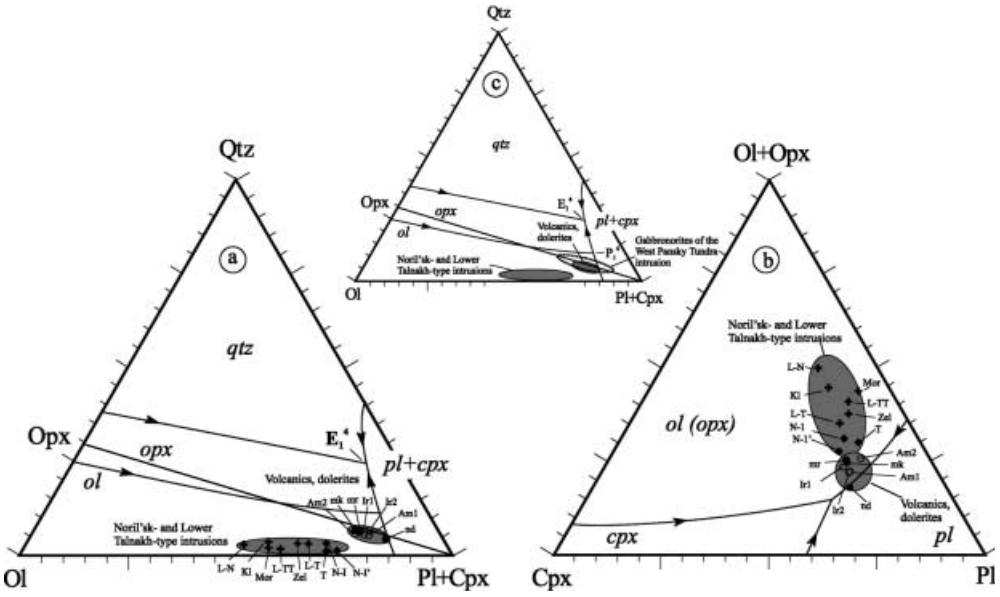

Fig. 5a–c. Projection planes of the isobaro-isoplethic section Ol–Cpx–Pl–Qtz showing fields with average compositions of the Nori'sk- (T, N-I, N-I') and Lower Talnakh-type (L-N, L-T, Kl, Mor, L-TT, Zel) intrusions, the Irbinsky (Ir1 and Ir2) and Ambarninsky (Am1 and Am2) dolerites intrusions, and average compositions of the nd, mr, and mk volcanic formations. Analytical data are listed in Table 6. Intrusions: *T* Talnakh; *N-I* Noril'sk I; *N-I'* Eastern Noril'sk branch of the Noril'sk intrusion; *L-N* Lower Noril'sk; *L-T* Lower Talnakh; *Kl* Klukvenny; *Mor* Morongo; *L-TT* Lower Tulaek-Taassky; Zel, Zelyonaya Griva. Formations: *nd* Nadezhdinsky; *mr* Morongovsky; *mk* Mokulaevsky. Note that a field with average compositions of the intrusions lies close to the critical Ol–Cpx–Pl plane of silica undersaturation whereas that of volcanic formations are located near to the critical Opx–Cpx–Pl plane of silica saturation. Also shown **c** is a field of gabbronorites of the West Pansky Tundra layered intrusion taken from Latypov et al. (1999)

basalts will complete their crystallization at the tributary point P_1^4 except some silica-rich basalts of the nd Formation, which, upon further fractionation, can reach a quartz-bearing isobaric invariant point E_1^4. Thus, the overall order of the phase crystallization of basalts – Ol (1–2) → Ol + Pl (2–3) → Ol + Pl + Cpx (3–P_1^4) → Ol + Pl + Cpx + Opx (P_1^4) – with the exception of Cr-spinel, is very similar to that of the intrusions. However, the position of the basalts close to the critical plane of silica saturation implies that their crystallization at the tributary point P_1^4 must result in the nearly complete peritectic replacement of olivine by orthopyroxene. The rare occurrence of orthopyroxene in the basalts is most probably the consequence of a short crystallization time at the point P_1^4 because of kinetic reasons. Much of the silica needed for conversion of olivine into orthopyroxene likely remained within volcanic glass (5–30 vol% in the basalts), which was later subjected to complete opacitizition and chloritization (Distler and Kunilov 1994). An additional reason for the absence of orthopyroxene in the basalts of the Noril'sk region can result from the crystallization of basalts in conditions when the liquidus line dips below the 2-pyroxene solvus leading to stability of only single clinopyroxene. This is a rather common phenomenon for crystallization conditions of lavas and hypabyssal subplutonic bodies.

Discussion and conclusions

Our study has revealed a significant compositional difference between the parental magmas of the Noril'sk- and Lower Talnakh-type intrusions and flood basalts, with the first lying close to the silica-undersaturated plane Ol–Cpx–Pl and the second lying close to silica-saturated plane Opx–Cpx–Pl. According to Yoder and Tilley (1962) classification, these magmas can be defined as silica-undersaturated olivine basalt and saturated tholeiite, respectively. Thus, the plutonic equivalent of the parental magmas of the intrusions is olivine gabbro (or melagabbro) whereas that of the basalts is gabbronorite. It is noteworthy that the type of magma responsible for the formation of the Noril'sk- and Lower Talnakh-type intrusions belongs to a rather specific kindred of Opx-free or nearly Opx-free magmas. A good example of plutonic bodies formed from the magmas of this kindred is the Kiglapait intrusion (Morse 1979) and layered intrusions of the Duluth Complex, Minnesota (Miller and Ripley 1996). In contrast, the tholeiitic silica-saturated basalts, similar in composition to those of nd, mr, and mk Formations, are quite common in many flood basalts provinces (Zolotukhin and Al'mukhamedov 1991).

Despite similarity in order of phase crystallization of the parental magmas of the intrusions and basalts, phase equilibria relations clearly show that they are not linked by the liquid line of descent (Fig. 3). Consequently, these magmas cannot be considered as co-magmatic. It is common opinion among Russian geologists that picritic basalts of the Gudchihinsky Formation have co-magmatic relationships with the intrusions under study (e.g., Duzhikov and Strunin 1992, and references

therein). Trace and isotope data (Naldrett et al. 1995), together with a phase equilibria analysis (Latypov, in preparation) provide, however, no support for this idea. Thus, it is not inconceivable that the Noril'sk- and Lower Talnakh-type intrusions have no direct co-magmatic volcanics in the Noril'sk region at all. As for the tholeiitic silica-saturated basalts of nd, mr, mk, and some other Formations, their plutonic co-magmatites are most likely represented by the Irbinsky and Ambarninsky dolerite intrusions (Fedorenko et al. 1984). The normative composition of these dolerites is dominated by plagioclase, clinopyroxene, and orthopyroxene components (Table 6). As a result, their average compositions fall within the field of the flood basalts on the projection planes (Fig. 5a, b) and on the Mg#-An(norm) plot (Fig. 6). The principal modal silicates of the dolerites are plagioclase (35–60%), clinopyroxene (15–55%), and minor amount of olivine (1–14%). As is the case with the basalts, the rare occurrence of orthopyroxene is likely related to a rather high content of silica-rich mesostasis (10–20%), composed presently of chlorite, actinolite, biotite, albite, and quartz.

The foregoing provides strong support to the conclusion of Czamanske et al. (1994) that the magmas, which produced the ore-bearing intrusions do not directly correspond to those parental to any of the erupted basalts. Therefore, the current model of intrusions as lava conduits (Naldrett at al. 1995), despite the fact that it does give a reasonable explanation for many perplexing aspects of the Noril'sk-type intrusions, cannot be regarded any longer as a satisfactory one. Some other mechanisms, which would be capable to account for an abnormally high ratio of the sulfides to the volume of silicate in the ore-bearing intrusions, are probably needed. Obviously, at the present state of investigation, it is reasonable to remain open-minded about the ore-forming and ore-emplacement processes in the Noril'sk region, which are as yet poorly constrained (Czamanske et al. 1994). It is reasonably safe to conclude that, however, the evidence for the non-co-magmatic relationship between basalts and intrusions suggests that the association of the very sulfide-rich intrusions with a large volume of chalcophile element-depleted basalts of nd_1 and nd_2 subformations in the Noril'sk region is likely coincidental rather than of genetic significance. The only possibility for the genetic relation is to assume that sulfides were initially precipitated from a melt parental for the basalts of nd_1 and nd_2 subformations somewhere in the crustal reservoir and then accidentally entrained by rising magma parental for the ore-bearing intrusions. This is improbable, however, in view of the tight relation between the ores and their host intrusions that have been established by lead and osmium-isotope studies (Czamanske et al. 1994). On this ground, it seems misleading to use the presence of magmatic formations depleted in Cu, Ni, and PGEs as a regional criteria in the prospecting for sulfides deposits in the flood basalts provinces (Fedorenko 1994a).

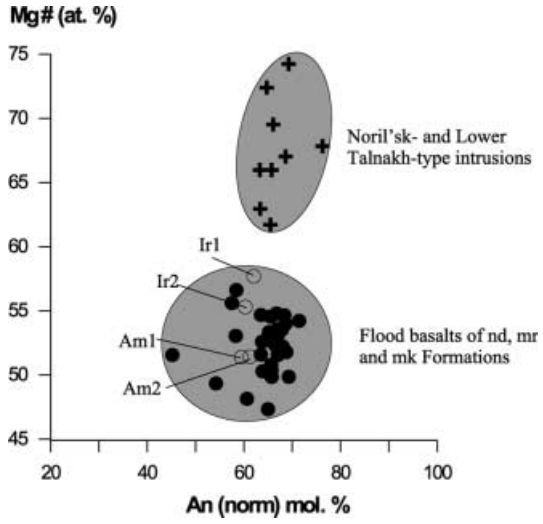

Fig. 6. Diagram Mg#–An(norm) illustrating the average compositions of the Nori'sk- and Lower Talnakh-type intrusions, the Irbinsky (Ir1 and Ir2) and Ambarninsky (Am1 and Am2) dolerite intrusions, and average compositions of the nd, mr, and mk volcanic formations. An(norm) = 100*An/(An + Ab), Mg# = 100*Mg/(Mg + Fe^{2+} + Fe^{3+}). Analytical data are listed in Tables 3, 4, 5 and 6

Acknowledgements I wish to express great thanks to V.A. Fedorenko for providing me with numerous valuable publications and analytical data containing separate determination of FeO and Fe_2O_3 without which it would have been impossible to calculate CIPW norms. The work essentially benefited from discussion with and constructive comments by V.A. Fedorenko and G.K. Czamanske. M.I. Dubrovskii read the manuscript, and his insightful comments are gratefully acknowledged. S.A. Morse is thanked for his constructive reviews of several versions of the paper. I also thank I. Carmichael for his editorial input. Editing by Stacy Saari led to significant improvement in the wording of the text. The research was supported by grants from Thule Institute of the University of Oulu and the Center for International Mobility (CIMO, Helsinki).

Appendix

Appendix A. Abbreviations used in the paper and tables

Pl plagioclase; *Ol* olivine; *Opx* orthopyroxene; *Cpx* clinopyroxene; *Qtz* quartz; *Cr-sp* Cr-spinel; *Mgt* titanomagnetite; *Fo* forsterite; *Fa* fayalite; *Di* diopside; *Hd* hedenbergite; *Ab* albite; *An* anorthite; *cc* calcite; *ap* apatite; *ilm* ilmenite; *pr* pyrite; *or* orthoclase; *en* enstatite; *fs* ferrosilite; *ne* nepheline; *mg#* Mg/(Mg + Fe); *mg#* ratio; *An = 100*/(An + Ab)* anorthite content of plagioclase; *L* melt; *E* eutectic point; *P* tributary point.

Appendix B. Projection planes of the phase diagram Ol–Cpx–Pl–Qtz

One of the planes runs through invariant points E_1^4 – Opx + Cpx + Pl + Qtz + L and P_1^4 – Ol + Opx + Cpx + Pl + L, and the Qtz–Ol join. The resulting tri-

angle Ol–Qtz–(Cpx + Pl) reflects the main changes in phase equilibria of the isoplethic section: the position of invariant points and the crystallization surfaces of phase associations with Qtz and Ol relative to the Opx–Cpx–Pl plane. The points of rock composition are plotted onto this projection by the conventional method, with the sum of wt% Ol + Qtz + Cpx + Pl (or Opx + Qtz + Cpx + Pl) brought to 100%. In doing this, it is necessary to recalculate Opx to Ol + Qtz. An alternative way of plotting is possible. Assemblages with Qtz are plotted onto the triangular Opx–Qtz–(Cpx + Pl), and those with Ol onto Opx–Ol–(Cpx + Pl), the scale of each triangular area being adhered to.

The second plane is a projection from the apex Qtz to a boundary plane Ol–Cpx–Pl. It reflects the relationships between Pl and Cpx, which are shown as a sum in the first projection. It is possible to plot compositional points onto this plane without considerable distortion by bringing the sum (Ol + Opx) + Cpx + Pl to 100%. By the position of composition points on the two projections planes it is easy to imagine their position relative to the topology elements of the diagram in the volume of a tetrahedron.

References

Brooks CK (1976) The Fe_2O_3/FeO ratio of basalt analyses: an appeal for a standardized procedure. Bull Geol Soc Denmark 25:117–120

Czamanske GK, Wooden JL, Zientek ML, Fedorenko VA, Zen'ko TE, Kent J, King B-SW, Knight RJ, Siems DF (1994) Geochemical and isotopic constraints on the petrogenesis of the Noril'sk–Talnakh ore-forming system. Proceedings of the Sudbury–Noril'sk Symposium. Ontario Geol Surv Spec Publ 5:313–342

Czamanske GK, Zen'ko TE, Fedorenko VA, Calk LC, Budahn JR, Bullock JH Jr, Fries TL, King B-SW, Siems DF (1995) Petrographic and geochemical characterization of ore-bearing intrusions of the Noril'sk type, Siberia; with discussion of their origin. Resour Geol Spec Issue 18:1–48

Distler VV, Kunilov VE (1994) Geology and ore deposits of the Noril'sk region. VII International Platinum Symposium Guidebook, Geoinformmark, Moscow

Distler VV, Smirnov AV, Grokhovskaya TL, Philimonova AA, Muravizkaya GN (1979) The stratification, cryptic variation and the formation of the sulfide mineralization of the differentiated trap intrusions. In: Smirnov VI (ed) The formation of the magmatic ore deposits. Nauka, Moscow, pp 211–269

Dubrovskii MI (1993) Physicochemical ($P(H_2O)$–T–*X*) models for the crystallization of magmatic olivine-normative rocks with a standard alkalinity. Nauka, St. Petersburg

Dubrovskii MI (1998) Differentiation trends of the standard alkalinity olivine-normative magmas and corresponding rock series. Kola Science Center, Apatity

Duzhikov OA, Distler VV (1992) Geology and metallogeny of sulfide deposits, Noril'sk region, USSR. Soc Econ Geol Spec Publ, vol 1

Duzhikov OA, Strunin BM (1992) Geological setting and general characteristics. In: Dushikov OA, Distler VV (eds) Geology and metallogeny of sulfide deposits, Noril'sk region, USSR. Soc Econ Geol Spec Publ 1:1–60

Ehlers EG (1972) The interpretation of geological phase diagrams. Freeman, San Francisco

Fedorenko VA (1994a) Evolution of magmatism as reflected in volcanic sequence of the Noril'sk region. Proceedings of the Sudbury–Noril'sk Symposium. Ontario Geol Surv Spec Publ 5:171–183

Fedorenko VA (1994b) Model of genetic relationship between flood basalts, ore-bearing intrusions and Cu–Ni–Pt ores in the Noril'sk region, NW Siberian platform, Russia, abstr 26. VII Int Platinum Symposium, Moscow

Fedorenko VA, Stifeyeva GT, Makeyeva LV, Sukhareva MS, Kuznetsova NP (1984) Mafic and alkaline-mafic intrusions of the Noril'sk region as being co-magmatic to the effusive formations. Soviet Geol Geophys 6:56–65

Godlevsky MN (1959) Traps and ore-bearing intrusions of the Noril'sk region. Gosgeoltechisdat, Moscow

Korzhinskii DS (1959) Physicochemical basis for analysis of the paragenesis of mineral. Consultants Bureau Inc, New York

Latypov RM, Mitrofanov FP, Alapieti TT, Kaukonen RJ (1999) Petrology of upper layered horizon (LLH) of West-Pansky intrusion, Kola Peninsula, Russia. Russian Geol Geophys 40:1434–1456

Lightfoot PC, Naldrett AJ (1994) Proceedings of the Sudbury–Noril'sk symposium. Ontario Geol Surv Spec Publ, vol 5

Lightfoot PC, Naldrett AJ, Gorbachev NS, Doherty W, Fedorenko VA (1990) Geochemistry of the Siberian trap of the Noril'sk area, USSR, with implications for the relative contributions of crust and mantle to flood basalt magmatism. Contrib Mineral Petrol 104:631–644

Lightfoot PC, Hawkesworth CJ, Hergt J, Naldrett AJ, Gorbachev NS, Fedorenko VA, Doherty W (1993) Remobilization of the continental lithosphere by a mantle plume: major-, trace-element, and Sr-, Nd-, and Pb-isotope evidence from picritic and tholeiitic lavas of the Noril'sk District, Siberian Trap, Russia. Contrib Mineral Petrol 114:171–188

Likhachev AP (1965) The role of the leucocratic gabbro in the formation of the ore-bearing differentiated intrusions of the Noril'sk region. PhD Thesis, Moscow University

Likhachev AP (1977) The conditions, which determined the formation of the trap magmas in the NW part of the Siberian platform. Proc All-Russian Mineral Soc 5:594–605

Likhachev AP (1994) Ore-bearing intrusions of the Noril'sk region. Proceedings of the Sudbury–Noril'sk symposium. Ontario Geol Surv Spec Publ 5:185–201

Marakushev AA, Fenogenov AN, Emel'yanenko PF (1982) Genesis of layered intrusions of the Noril'sk type. Vestnik Moscow Univ Geol Ser 1:3–19

Miller JD, Ripley EM Jr (1996) Layered intrusions of the Duluth Complex, Minnesota, USA. In: Cawthorn RG (ed) Layered intrusions. Developments in petrology, vol 15. Elsevier Science BV, Amsterdam, pp 257–301

Morse SA (1979) Kiglapait geochemistry II: petrography. J Petrol 20:591–624

Naldrett AJ (1994) The Sudbury–Noril'sk symposium, an overview. Proceedings of the Sudbury–Noril'sk Symposium. Ontario Geol Surv Spec Publ 5:3–8

Naldrett AJ (1997) Key factors in the genesis of Noril'sk, Sudbury, Jinchuan, Voisey's Bay and other world-class Ni–Cu–PGE deposits: implications for exploration. Aust J Earth Sci 44:283–315

Naldrett AJ, Lightfoot PC, Fedorenko VA, Doherty W, Gorbachev NS (1992) Geology and geochemistry of intrusions and flood basalts of the Noril'sk region, USSR, with implications for the origin of the Ni–Cu ores. Econ Geol 87:975–1004

Naldrett AJ, Fedorenko VA, Lightfoot PC, Kunilov VI, Gorbachev NS, Doherty W, Johan Z (1995) Ni–Cu–PGE deposits of Noril'sk region, Siberia: their formation in conduits for flood basalt volcanism. Inst Mining Metall 104:B18–B36

Nekrasov IY, Gorbachev NC (1978) Physicochemical conditions of formation of the differentiated intrusions and copper-nickel ores of the Noril'sk type. Trans Physicochem Petrol 7:92–123

Osborn EF, Tait DB (1952) The system diopside–forsterite–anorthite. Am J Sci Bowen Vol 250(A):413–433

Rad'ko VA (1991) Model of dynamic differentiation of intrusive traps in the northwestern Siberian platform. Soviet Geol Geophys 32:15–20

Ricci JE (1951) The phase rule and heterogeneous equilibrium. Van Nostrand, Toronto
Ryabov VV (1992) Olivines of the Siberian traps as indices of petrogenesis and ore formation. Nauka, Novosibirsk
Schreinemakers FA (1965) Papers by F.A. Schreinemakers, 1, 2. (1912–1925). Pennsylvania, Pennsylvania State University
Yoder HS, Tilley CE (1962) Origin of basalt magmas: an experimental study of natural and synthetic rock systems. J Petrol 3:342–532
Zen'ko TE (1983) Mechanism of formation of the Noril'sk ore-bearing intrusions. Izvestia Acad Sci USSR Geol Ser 11:21–39
Zolotukhin VV, Al'mukhamedov AI (1991) Basalts of the Siberian Platform: distribution, mineral composition and mechanism of formation. In: Traps of Siberia and Deccan: similarities and differences. Nauka, Novosibirsk, pp 7–39
Zolotukhin VV, Ryabov YuA, Vasiliev YR, Shatkov VA (1975) Petrology of the Talnakh ore-bearing differentiated trap intrusion. Nauka, Novosibirsk